Reprinted from the Journal of the American Ceramic Society, Vol. 70, No. 4, April 1987

Crack-Interface Grain Bridging as a Fracture Resistance Mechanism in Ceramics: I, Experimental Study on Alumina

PETER L. SWANSON,* CAROLYN J. FAIRBANKS, BRIAN R. LAWN,* YIU-WING MAI,* and BERNARD J. HOCKEY

Ceramics Division, National Bureau of Standards, Gaithersburg, Maryland 20899

Direct microscopic evidence is presented in support of an explanation of *R*-curve behavior in monophase ceramics by grain-localized bridging across the newly formed crack interface. In situ observations are made of crack growth in tapered cantilever beam and indented flexure specimens of a coarse-grained alumina. The fractures are observed to be highly stable, typical of a material with a strongly increasing resistance characteristic, but are discontinuous at the microstructural level. Associated with this discontinuity is the appearance of overlapping segments in the surface fracture trace around bridging grains; the mean spacing of such "activity sites" along the trace is about 2 to 5 grain diameters. These segments link up with the primary crack beneath the specimen surface, and continue to evolve toward rupture of the bridge as fracture proceeds. The bridges remain active at large distances, of order 100 grain diameters or more, behind the crack tip. Scanning electron microscopy of some of the bridging sites demonstrates that secondary (interface-adjacent) microfracture and frictional tractions are important elements in the bridge separation process. Evidence is sought, but none found, for some of the more popular alternative models of toughening, notably frontal-zone microcracking and crack-tip/internal-stress interaction. It is suggested that the crack-interface bridging mechanism may be a general phenomenon in nontransforming ceramics.

I. Introduction

THERE is a growing realization that the crack resistance properties of ceramics have an intrinsic size dependence.[1] At crack sizes small in relation to the microstructure the toughness has values characteristic of bulk cleavage (transgranular) or grain boundary (intergranular) energies. At large crack sizes the toughness tends to somewhat higher, limiting values characteristic of the polycrystalline aggregate. The toughness function connecting these two extremes in crack size is the so-called "*R*-curve" function, after the rising crack resistance curves originally found for metals.[2] Such *R*-curve behavior is of great interest in the case of engineering ceramics, for both the structural designer, who needs to know the toughness characteristic in specifiable flaw size ranges, and the materials processor, who seeks a basis for tailoring new and superior materials.

Despite this increasing awareness of the importance of microstructurally related size effects, there have been remarkably few attempts at definitive identification of underlying crack resistance mechanisms. A notable exception is in the zirconia-based ceramics, where transformation toughening is now unequivocally established as a principal factor.[3-5] The transformation events are generally taken to be confined within a "process zone" about the advancing crack tip, in analogy to the plastic zone responsible for the *R*-curve behavior of metals. However, important as it is as a mode of crack impedance, transformation toughening is currently restricted to a select few ceramics and does not operate in "simple" monophase materials like aluminas. Crack size effects in these latter materials have been attributed to several alternative causes, with virtually no direct experimental substantiation. Perhaps the most widely quoted of these is the proposal of a frontal *microcrack* cloud, in which discrete microfractures act as effective energy sinks in the field of the primary crack.[6,7] Another proposal is that an advancing crack tip is progressively impeded via direct interactions with locked-in internal stresses (e.g., thermal expansion mismatch stresses).[8] Other possibilities that have been considered include crack restraint by pinning and bowing[9] and by deflection and twisting,[10] although these are noncumulative mechanisms; they do not have provision to account for the remarkably long crack size range over which the *R* curve rises in many materials.[1]

Which of the above mechanisms, if any, predominates in the *R*-curve behavior of aluminas and other nontransforming ceramics? The current literature relating to this question is based almost exclusively on the capacity of theoretical models to match measured fracture mechanics (e.g., applied load vs crack size) data. The question of whether or not the proposed mechanisms actually operate in the assumed fashion is not directly addressed in this literature; support is provided only by circumstantial evidence from limited postfailure examinations of fracture specimens. However, there is one set of observations, by Knehans and Steinbrech,[11] which allows us to narrow down the possibilities. They grew cracks through several millimeters in alumina test specimens, and found strong rising *R* curves. Then they removed material adjacent to the walls *behind* the crack tip by sawcutting, taking care to leave intact the immediate region *at* the tip. On restarting the crack, the resistance reverted immediately to the base of the *R* curve. The unmistakable implication was that the toughening processes must operate in the wake of the advancing tip. Of the mechanisms considered thus far, it is that of distributed microcracking which is most compatible with this notion of a wake effect; indeed, the Knehans and Steinbrech experiment has been cited as evidence for the microcracking model.[7]

However, Knehans and Steinbrech raised another possibility, that the source of the rising resistance may lie in some physically restraining force across the newly formed crack interface. This alternative proposal had received only passing mention in the preceding ceramics literature.[12,13] Knehans and Steinbrech have since taken their case further, arguing specifically in favor of a grain interlocking mechanism.[14,15] The idea of an interfacial restraint is not the exclusive domain of the ceramics community; it has been developed even more strongly in concrete[16,17] and rock mechanics,[18,19] although the detailed micromechanics of the actual separation processes are hardly better understood. Thus it would seem that the key to improving the toughness of nontransforming ceramics could depend primarily on events which occur behind rather than at or ahead of the advancing crack. Clearly there are important implications here in the microstructural design of ceramic materials.

The present work is directed to the development of a crack resistance model incorporating the essential elements of the inter-

Presented at the 88th Annual Meeting of the American Ceramic Society, Chicago, IL, April 30, 1986 (Basic Science Division, Paper No. 166-B-86). Received April 16, 1986; revised copy received September 2, 1986; approved October 14, 1986.

Supported by the U.S. Air Force Office of Scientific Research; support for P. L. S. provided by an NRC Postdoctoral Fellowship and support for Y.-W. M. provided by the NBS Guest Worker Program.

*Member, the American Ceramic Society.

*On leave from the Department of Mechanical Engineering, University of Sydney, N.S.W. 2006, Australia.

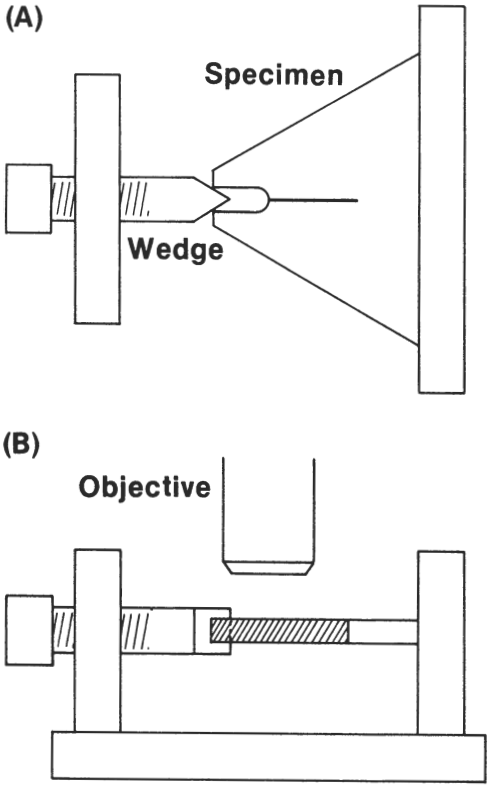

Fig. 1. Schematic of tapered double cantilever beam test specimen used to observe crack growth during loading: (*A*) top view; (*B*) side view. Specimen cut from triangular slab, 12-mm edge length and 2-mm thickness, to produce crack 7 mm long. Starter notch length 300 μm, radius 100 μm. Wedge angle 60°.

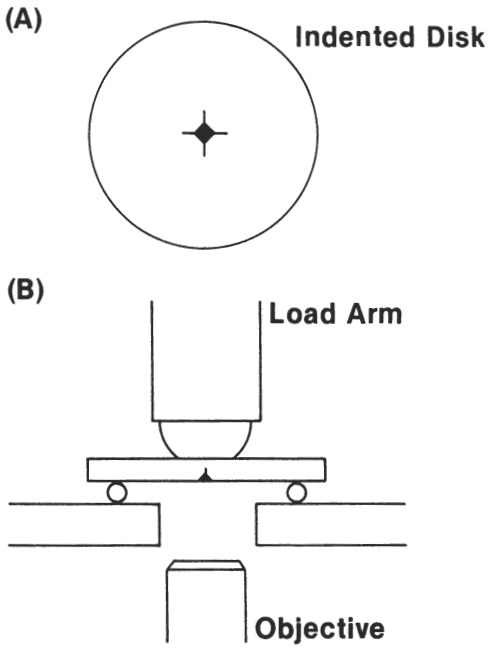

Fig. 2. Schematic of indentation flaw test used to observe radial crack evolution to failure: (*A*) plan view, showing Vickers flaw on tensile surface; (*B*) side view, showing flexure system. Specimen dimensions 25-mm diameter by 2-mm thickness. Biaxial loading, 2-mm-radius punch on 10-mm-radius (3-point) support.

facial restraint concept. It is in two parts. Part I describes experimental observations of controlled crack growth in a coarse-grained alumina with strong *R*-curve behavior. A critical feature of these experiments is the facility to follow the crack response along its entire length while the driving force is being applied. We confirm the presence of grain-localized "bridges" across the crack interface, over large distances (several millimeters) behind the tip. Part II deals with quantitative aspects of the *R*-curve behavior, by a formulation of the bridging concept in terms of theoretical fracture mechanics. In this endeavor we borrow from analogous treatments in the fiber-reinforced composite and concrete literature. Our analysis does not aspire to a complete understanding of the physical ligamentary rupture process, but nevertheless establishes a sound mechanical framework for characterizing the crack resistance properties.

Before proceeding, it is well that we should draw attention to a recent study on the strength properties of ceramic specimens containing indentation flaws.[20–22] Indeed, some of the issues raised in that study provided a strong motivation for the present work. There, the idea was to investigate the fracture size range between the extremes of the microscopic flaw and the macroscopic crack by systematically varying the indentation load from specimen to specimen. It was found that on reducing the indentation flaw size the corresponding strength did not increase indefinitely, as required by ideal indentation fracture theory (i.e., theory based on the notion of an invariant toughness), but tended instead to level off at a strength characteristic of the intrinsic microstructural flaws. This response was attributed to the influence of *R*-curve behavior. Importantly, the strength plateau at small flaw sizes was seen in three groups of ceramics, aluminas, glass-ceramics, and barium titanates, indicating a certain generality in the *R*-curve phenomenon. Also, the magnitude of the effect was in some cases considerable, amounting to an effective increase in toughness of more than a factor of 3 over a crack size range of some tens of grain sizes or more. In that earlier study[20] the microstructural element was introduced into the fracture mechanics in a somewhat phenomenological manner: here we seek to place the fracture mechanics on a firmer footing by relating this element more closely to identifiable crack restraint mechanisms. Accordingly, a detailed analysis of indentation fracture data in terms of the bridging concept may be foreshadowed as a future goal of our work.[23]

II. Experimental Procedure

It was decided in this work to focus on one material, a nominally pure, coarse-grained alumina.† We have already made allusion to the implied generality of the *R*-curve phenomenon (Section I); our choice is intended to meet the requirement of a "representative" material, but at the same time one which exhibits the *R* curve to particularly strong effect. (For quantitative measures of the pertinent *R* curve the reader is directed to the VI-labeled curves in Figs. 4 and 10 in Ref. 20, Figs. 6 and 7 in Ref. 1, and Figs. 1 and 3 in Ref. 22.) The relatively large microstructure of our material (mean grain diameter 20 μm) also lends itself to in situ experimentation using ordinary means of microscopic observation. In certain instances where it was deemed useful to run comparative tests on specimens *without* the influence of microstructure, sapphire was used as a control material.

As indicated, a major feature of our experimental procedure is the facility to monitor the evolution of fracture during the application of stress. Accordingly, direct observations were made of the crack growth by optical microscopy, using the two loading configurations shown in Figs. 1 and 2. The specimens were surface-relief polished with 0.3-μm Al_2O_3 powder to delineate the coarser grain boundary structure. In some cases a thermal etch pretreatment at (1050°C for 2 h) was used to enhance fine details in

†Vistal grade, Coors Porcelain Co., Golden, CO.

this structure. An important element of our experimental philosophy here is that, by virtue of the enhanced stabilization in crack growth which attends strong R-curve behavior,[1] we may hope to observe critical events which in conventional postfailure analysis (or even in interrupted tests) might pass unnoticed.

The first of the test configurations, Fig. 1, is a modification of the familiar double cantilever beam specimen. Generally, the regular rectangular beam geometry is retained for *quan*titative evaluation of the R-curve behavior (Part II). Here, however, a tapered geometry was used, width increasing in the direction of ultimate crack propagation. The main crack was started at a sawcut notch by inserting a metal wedge. Subsequent crack extension could be controlled via a micrometer drive system, to which the wedge was fixed. The whole system was attached to the stage of an optical microscope to allow for continuous monitoring of the crack evolution. Pertinent dimensions of the test geometry are included in the caption to Fig. 1.

The second configuration, Fig. 2, simulates the controlled flaw test used previously to infer R-curve behavior from strength data (Section I). A Vickers diamond was used to introduce an indentation flaw at the center of a disk flexure specimen. The disk was then loaded axially in a circular-flat on three-ball-support fixture,[24] with the indentation on the tension side. Again, the entire fixture was attached to a microscope stage for in situ viewing of the crack evolution. A video recording unit was particularly useful in interpreting some of the more subtle features observed with this configuration. Reference is made to Fig. 2 for relevant test geometry dimensions.

Some additional, static observations were made on the above specimens to add weight to our ensuing case. For example, in the event of toughening associated with a frontal microcrack cloud, one might anticipate some detectable surface distortion either ahead or in the wake of the primary crack tip. Accordingly, surface profilometry scans were taken perpendicular to the crack traces on some of the cantilever specimens. The cantilever configuration was more convenient in this regard because the entire wedge-loading fixture could be transferred onto the profilometer stage, thereby allowing the crack to be examined without unloading. Also, anticipating that we might need to look more closely at events at the level of the grain size *or below,* some of the unloaded disk specimens were examined by scanning electron microscopy.

III. Results

(1) General Observations

Our initial examinations of the fracture patterns produced in the alumina test specimens revealed some interesting general features. The clearest and most immediate indication that we were dealing with a crack-interface effect was that, after "failure" (as marked by a sudden propagation of the cracks to the edges of the specimen), the fractured segments tended to remain intact. An additional force was required to separate the pieces completely. This was our first clue that the walls behind an advancing tip must indeed be restrained by some remnant forces acting across the interface.

Closer surface inspections along the crack traces at various stages of propagation soon helped to reinforce this last conviction. The fracture in our material was predominantly intergranular, as previously reported.[20,21] There were signs of some "secondary activity" adjacent to the walls of the otherwise primary crack interface, but never further distant than one or two grain diameters from this interface. It will be our aim in the following sections to confirm that this interface-related activity is a manifestation of a grain-localized ligamentary rupture process, and not of some relaxation effect associated with the wake of an advancing microcrack cloud.

(2) Cantilever Beam Experiments

The in situ observations of fracture in the tapered cantilever beam specimens (Fig. 1) were carried out while carefully and slowly driving in the mouth-opening wedge. These observations were all made in air, so that some rate effects were apparent in the crack growth (although the velocities were usually much less than 10^{-5} m·s^{-1}). There was a tendency for the first stage of fracture to occur suddenly over a distance of several grain diameters from the starter notch tip. "Pop-in" behavior of this kind is not uncommon in notched specimens, of course; in such cases the initial fracture response can be influenced strongly by the local notch configuration. However, discontinuous crack growth was also commonly observed in the subsequent loading, over distances as small as one or two grains. There is the suggestion here of an element of discreteness in the mechanics which ultimately underlies the R-curve behavior.

Appropriately, attention was focused on regions of identifiable "activity sites" behind the advancing crack tip during monotonic loading to "failure." An example of the kind of observation made is shown in Fig. 3, a low-magnification reflected-light mosaic of a particular specimen at six successive stages of fracture. The field of view along the crack length covers the first 2 mm from the starter notch at left (not included in the figure). At final loading, stage VI in Fig. 3, the crack extends clearly across the full 7-mm length of the specimen, although again without separating into two parts. The areas labeled (*A*), (*B*), and (*C*) illustrate particularly clear examples of progressive crack-flank damage evolution through the loading sequence. These areas are magnified in Figs. 4 to 6 for closer scrutiny of the microstructural detail.

In zone *A,* Fig. 4, we can follow the formation and rupture of a single ligamentary bridge through all six stages. In stage I the surface fracture trace appears to be segmented about a large grain, as though the primary crack may have stopped and then reinitiated on a secondary front. However, on switching to transmitted light (e.g., see Fig. 7(*B*)) and focusing into the subsurface regions of the transparent material, the apparently isolated segments were found to connect together into a common crack interface. Hence the bridge is grain-localized in the projected fracture plane. On proceeding to stage II we note that the crack segments about the bridging grain have increased their overlap but have not yet linked up, although the detectable main tip is now some 0.75 mm distant. There is an indication of enhanced reflectivity beneath this same grain, indicating that the crack-segment overlap extends *beneath* as well as *along* the surface. By the time the primary tip has advanced more than 1.2 mm beyond the bridge, stage III, the upper crack segment appears to have linked up completely with the main fracture trace. This does not signify the final state of rupture, however, for there are signs of continued local crack activity around the grain of interest, notably at left, through stages IV and V. We point out that the primary crack tip is at least 2 mm, i.e., approaching 100 grain diameters, ahead of the bridge site. Finally, at stage VI, the lower crack associated with the original bridge appears to have closed up somewhat, perhaps reflecting the release of some interfacial frictional tractions.[‡]

Zone *B,* in Fig. 5, evolves in much the same way, but with certain of the above-mentioned features delineated more strongly. The initial crack segmentation, stage III, and subsequent linkup, stage IV, differ little in essence from that observed in zone *A*. However, the trace of the crack segment which runs *below* the bridging grain (and which, incidentally, would appear in stage III to be the more likely to lead to the ultimate rupture of the ligament) closes up much more abruptly and completely than its counterpart in zone *A*. Interfacial tractions persist on loading to stage V, as evidenced by the appearance of additional small-scale fissures about the separating grain. Examination in transmitted light during this stage revealed substantial subsurface activity. Even more dramatic indications of unrelieved tractions are evident from the postmortem configuration at stage VI. Final separation has occurred through virgin material, seemingly "avoiding" the incipient fracture paths apparent in the previous micrographs; a measure of the disruption caused by this final rupture is given by the extensive debris, visible as the region of highly diffuse reflection, lodged

[‡]Interfacial tractions and bridging by as-yet unruptured grains may *independently* provide traction across the nascent fracture surface. Distinction between these two potential sources of traction is not a principal concern here, owing to the experimental difficulties in resolving finer details in the subsurface damage processes.[19,25]

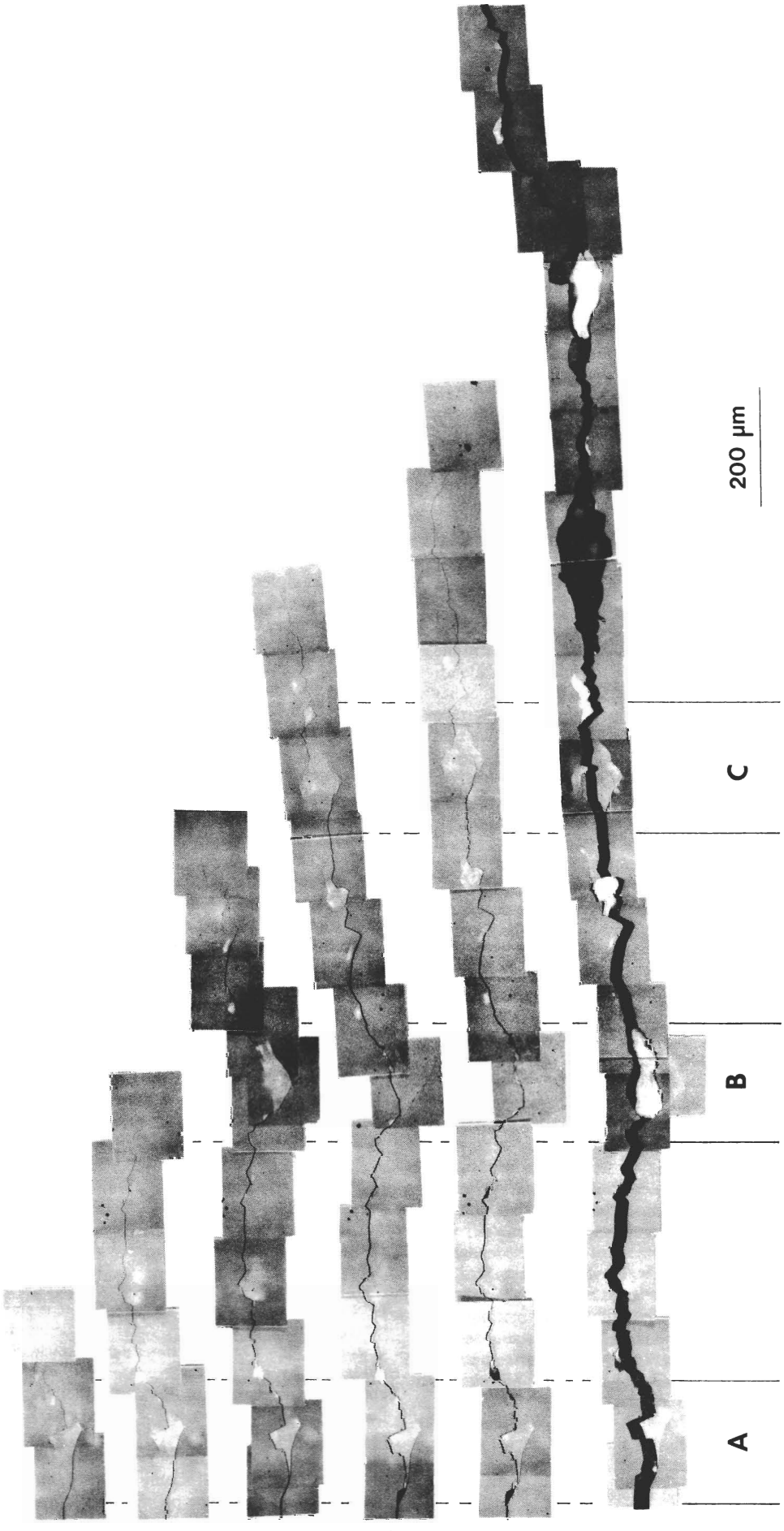

Fig. 3. Reflected light micrograph mosaic of crack evolution in tapered DCB specimen of alumina, shown at six stages of loading. Wedge remains inserted in notch (just out of field at left) in all stages.

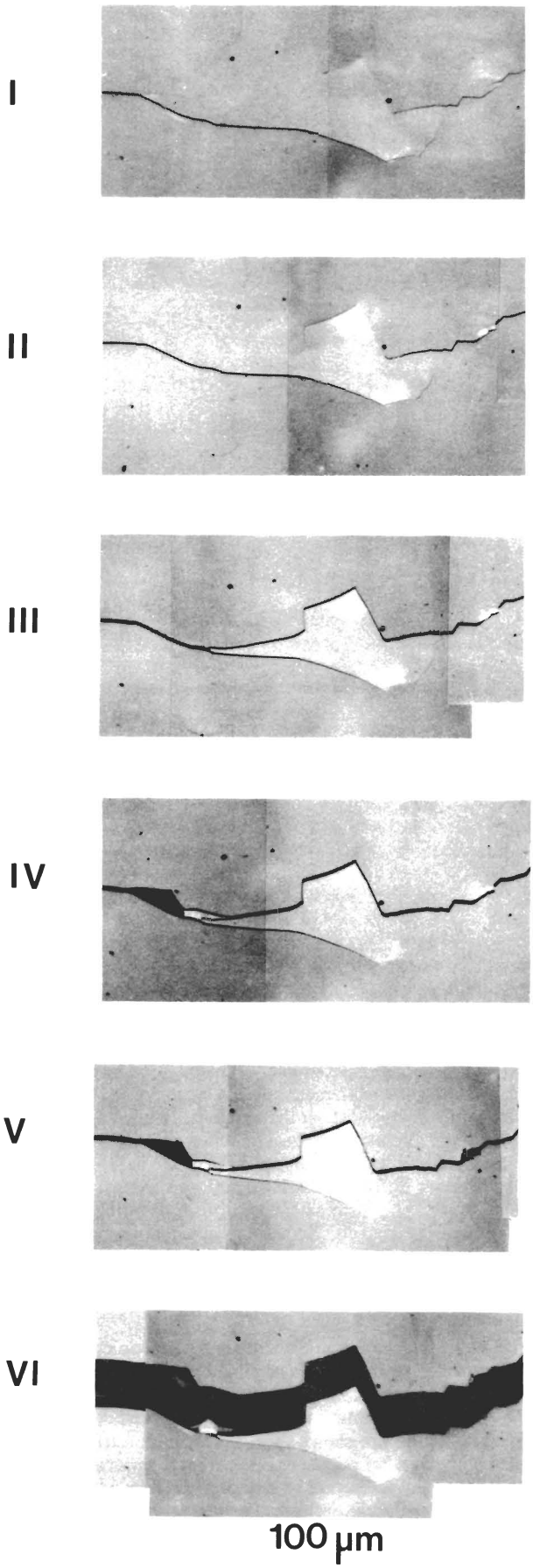

Fig. 4. Enlargement of zone *A* in Fig. 3, showing evolution of a grain bridging site from inception to failure. Persistence of interface-related secondary cracking is apparent through stage V.

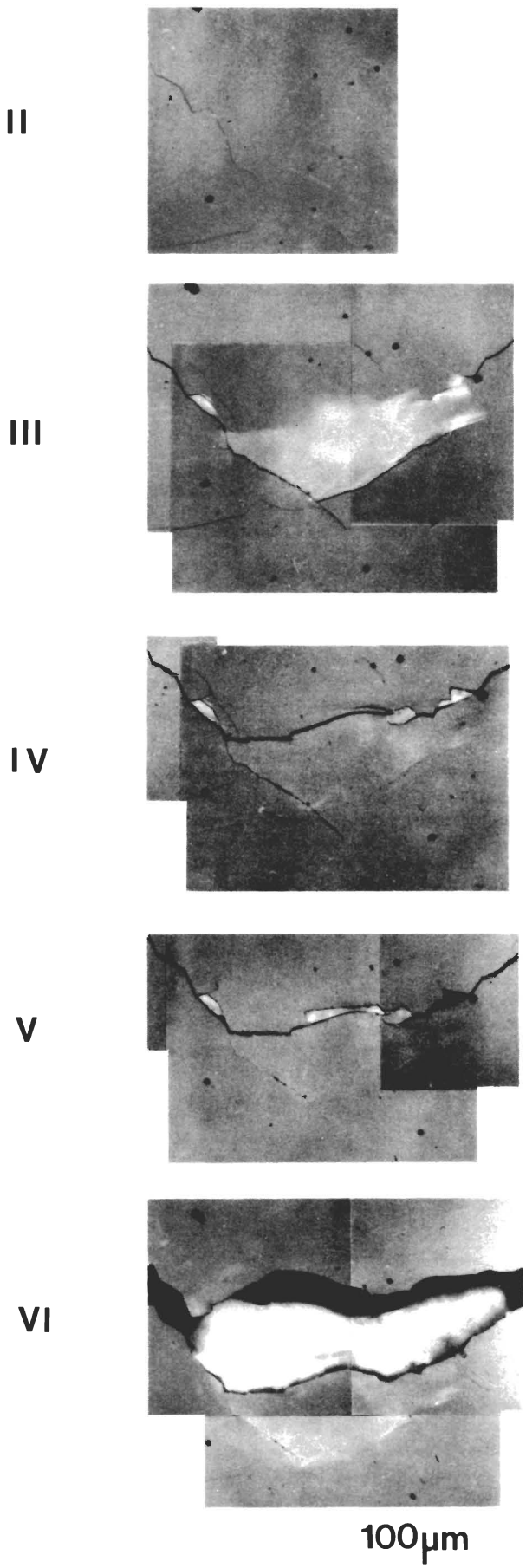

Fig. 5. Enlargement of zone *B* in Fig. 3. Note continually changing course of the local fracture path through the loading to failure.

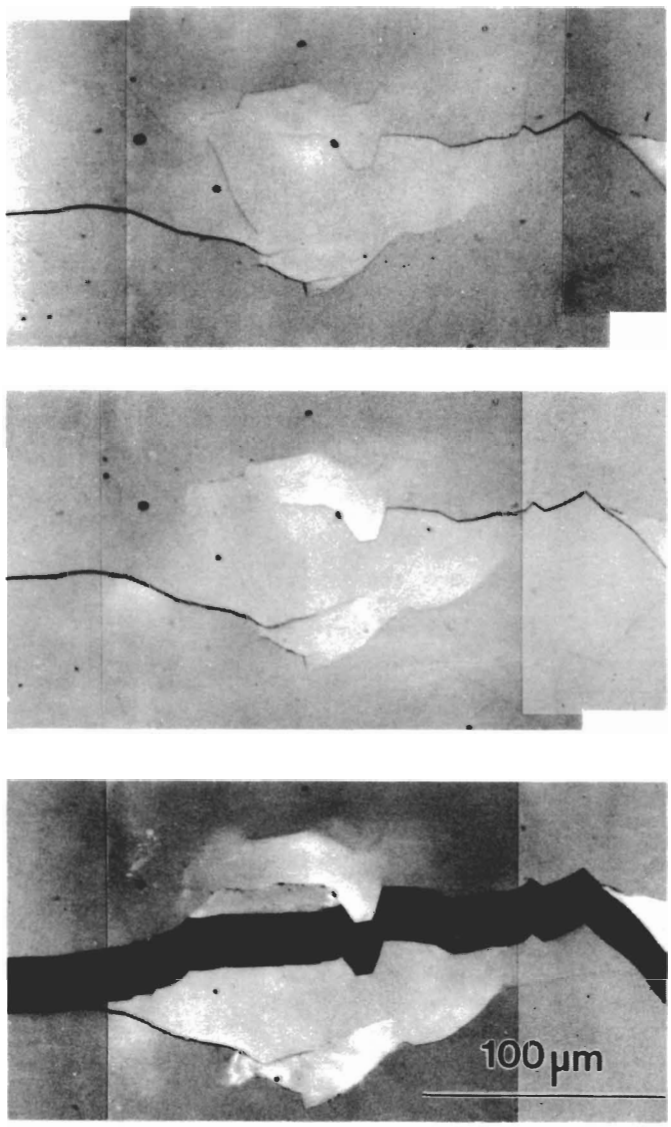

Fig. 6. Enlargement of zone *C* in Fig. 3. Substantial transgranular fracture accompanies the bridge rupture.

between the crack walls at the original bridge site.

Consider now the third area in Fig. 6, zone *C*. In the initial stage, IV, substantial microcrack overlap occurs, predominantly along grain boundaries, followed by transgranular microrupture *within* the initial span of bridging material, stage V. Again, the final rupture path largely ignores the previously formed, localized crack segments.

We note that at each bridge-rupture site (zones *A*, *B*, *C*) the cumulative amount of surface-exposed crack length is approximately *3 times* the shortest straight-line path through the bridging sites. Moreover, the total fracture surface area incorporates a significant amount of transgranular fracturing. The bridges clearly represent an intrinsically high-energy source of fracture resistance.

In choosing our examples above we have, for obvious reasons, focused on the most conspicuous sites, i.e., the sites involving the largest bridging grains. Higher magnification examinations of loaded crack systems such as that in Figs. 3 to 6 revealed a high density of smaller, but no less active, sites, particularly toward the fracture terminus. These were again evident as surface offset traces in reflection or subsurface scattering centers in transmission. It was thereby estimated that the mean separation between grain ligaments could be as low as 2 to 5 grain diameters.

With the realization that our microscopic observations were capable of detecting grain-scale microfractures while load was maintained, particularly in illumination by transmitted light, attention was turned to the region *ahead* of the primary crack terminus. Figure 7 shows typical micrographs of this region. In particular, evidence was sought which might point to the existence of a cloud of distributed microcracks about the terminus. In keeping with the popular notion of discrete microfracture initiation at or above some critical tensile stress level within the near crack field, we might expect to observe diffuse scattering within an extensive frontal microcrack zone.[6,7] No such extended diffuse scattering was ever detected in our experiments. Sometimes apparently unconnected surface traces were observed in the terminus region (e.g., as in Fig. 7(*B*)) but, like their segmented counterparts *behind* the tip, these invariably connected up at a depth of a grain diameter or so beneath the surface.

Further null evidence for an extended transverse microcracking zone was provided by the surface profilometer traces. These were taken perpendicular to the loaded crack configuration seen in stage IV, Fig. 3. The results of several scans, both ahead and behind the crack tip, are shown in Fig. 8. Minute surface detail associated with the relief polishing is apparent in the scans, but in no case is there any indication of a general dilation-induced uprising of material adjacent to the crack interface.

(3) Indentation-Strength Experiments

Direct observations were made of crack growth from Vickers indentation flaws during loading to failure (Fig. 2). An example of the final fracture pattern produced in this configuration is given in Fig. 9. We see that once the initial radial cracks traverse the central

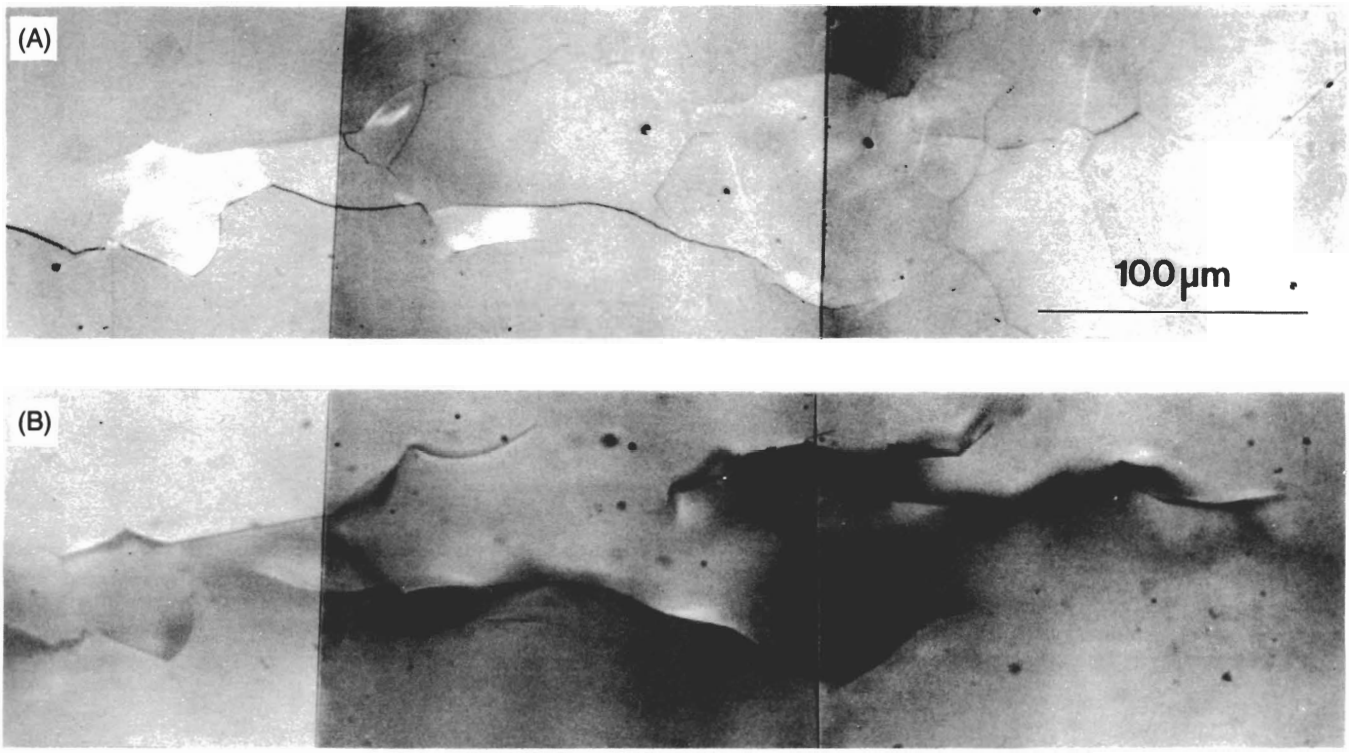

Fig. 7. Reflection (*A*) and transmission (*B*) micrographs of loaded DCB specimen (equivalent in growth to about stage IV in Fig. 3).

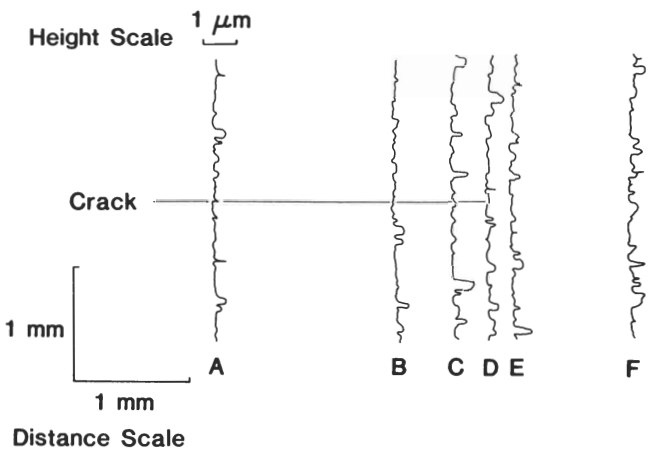

Fig. 8. Surface profilometer traces transverse to crack plane in loaded alumina DCB specimen. Detectable crack tip lies on trace *D*. Height scale on scan greatly magnified relative to distance scale. No surface uplift adjacent to crack walls is evident (diamond stylus radius $\simeq 1$ μm; horizontal position uncertainty ± 100 μm, vertical uncertainty <10 nm for long wavelength, i.e., $\gtrsim 10$ μm, topography variations).

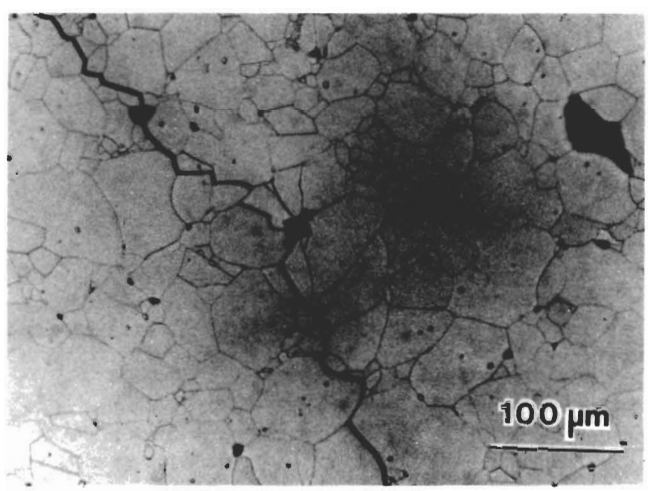

Fig. 9. Reflected light micrograph of a Vickers indentation site in a "fractured" alumina disk. Initial radial cracks from low-load (5 N) indentation arrest at first encounter with grain boundary, and grow discontinuously *along* boundaries as flexural stress is applied. Specimen thermally etched to reveal grain structure.

grains which encompass the indentation impression, the fracture proceeds primarily in the familiar intergranular mode. Once more, this fracture runs to the specimen extremities without causing complete separation.

One of our acknowledged goals here was to look in fine detail at the crack response *prior to* failure. Accordingly, the tests were run at slow stressing rates, in air, for greatest ease of observation. Typically, the time to failure was several minutes. At high indentation loads ($\gtrsim 100$ N), such that the scale of the starting radial cracks substantially exceeded that of the microstructure, the fracture showed an even stronger tendency to discontinuous evolution, over distances of a few grains or so, than noted in the cantilever beam experiments. Notwithstanding these discontinuities, the cracks were characterized by strong prefailure stability, sometimes extending to the edges of the 12.5-mm-radius disks without any sign of catastrophic growth. There is no doubt that local residual contact stresses contribute to this stability,[26] but only in part; comparative runs on sapphire (microstructure-free) specimens under identical test conditions show much smaller, i.e., $\ll 1$ mm, precursor stable growth prior to failure. It seems reasonable to conclude that the enhanced stabilization in the polycrystalline alumina is a direct manifestation of a rising R curve.[1]

At low indentation loads (1 to 10 N) the evidence for discontinuity in the stabilized crack growth was even more emphatic.

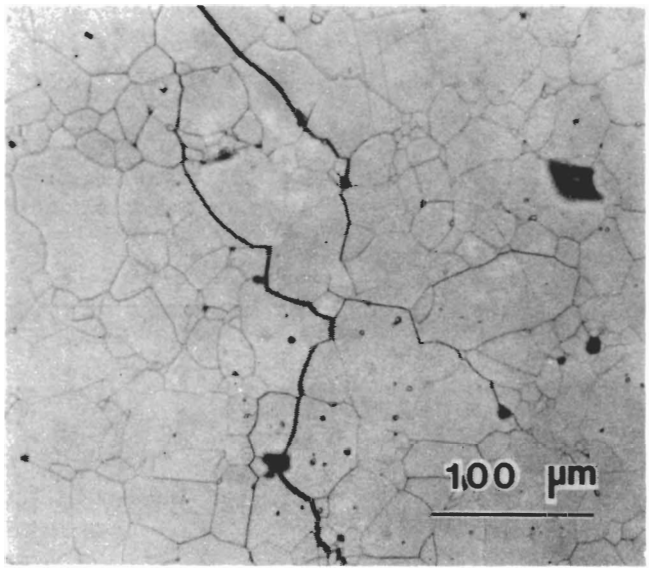

Fig. 10. Reflected light micrograph of a segmented radial crack in a partially fractured alumina disk.

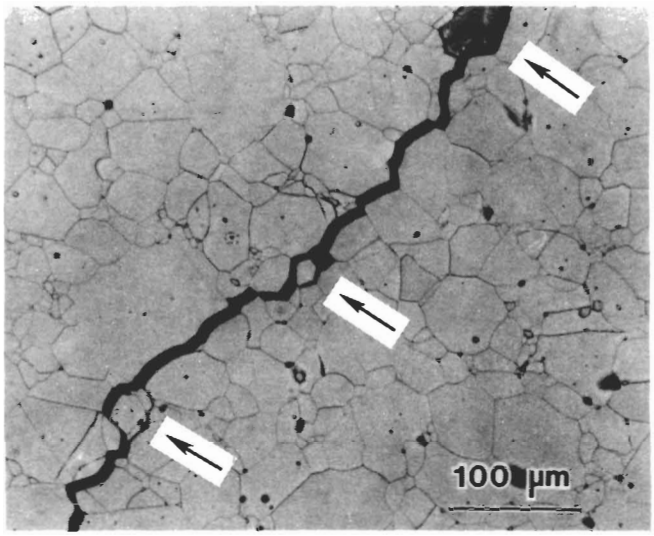

Fig. 11. Reflected light micrograph of portion of a radial crack in a fractured-but-intact alumina disk. Disturbance of some interface-adjacent grains is evident (arrows).

This is the region of the load-insensitive plateau in the strength data[20] referred to in Section I. The radial cracks seemed to remain "trapped" at the encompassing grain boundaries (see Fig. 9) during the flexural loading up to some critical level, at which point a sudden burst of growth ensued. This initial growth pattern was highly variable from specimen to specimen. In many cases the growth distance was small, of the order of grain dimensions, before arresting. Also, individual radial cracks tended to propagate independently, at different levels in the loading. We may liken this initial phase of the fracture evolution to the pop-in observed in the beam configuration (Section II(2)); however, now we can be certain that we are indeed observing an intrinsic property of the small-scale flaw and not some artifact due to the fracture (e.g., notch) geometry. On increasing the applied loading further these radial cracks continued to extend intermittently, but at an increasing jump frequency with respect to stress increment. Thus the "smoothness" in the approach to ultimate failure depended on the number of jumps activated during the loading. In some extreme cases the initial burst of crack propagation was so "energetic" as to take the stressed system spontaneously to failure.

It was also observed that the same kind of discontinuous crack growth and arrest occurred at prominent *natural* flaws in the alumina specimens. These flaws included grain pullout sites on imperfectly polished surfaces and internal fabrication pores. Occasionally such flaws provided the ultimate center of failure, most notably at the low end of the indentation load scale. There seemed little tendency for these competing sites to interact with each other, although inevitably neighbors would occasionally combine to produce an enlarged, yet still stable, composite crack.

Our observations of strong discontinuity and enhanced stabilization in the indentation-strength specimens turns our attention, as in the cantilever beam experiments, to events behind the growing crack tip. Essentially, our in situ examinations of the radial crack evolution to failure revealed the same kind of general grain-bridging features as described earlier in Figs. 4 to 6. Figure 10 shows an example of a particularly large bridging site behind the tip of an extended radial crack. Sites of this kind located as far back as the indentation impression corners remained active throughout the growth to failure, even in those specimens with millimeter-scale stable extensions, confirming that interface restraints act over distances on the order of 100 grains or more. The self-consistency of the grain separation patterns in the two specimen types examined here serves to allay any concern that we might be observing some test-geometry-specific artifact (although geometry effects can still be an important factor in the *R*-curve behavior; see Part II).

Some of the broken specimens remained intact to a degree which left much of the grain bridging debris trapped between the crack walls. An example is shown in Fig. 11. There are clear indications of loosening and dislodging of interface-adjacent grains along the crack trace. It appears from the way some of these disturbed grains are rotated about their centers that there are intense local tractions at work. In extreme cases the intensity of these tractions is sufficient to detach the grain completely, and with some energy to spare: in some of the in situ video recording sequences individual grains occasionally disappeared along the crack trace in a single frame interval (e.g., upper left of trace in Fig. 9). Such "pop-out" events invariably occurred as the applied loading was being increased, so the tractions cannot be attributed to spurious closure forces.

For more detailed investigation of the crack-interface events, specimens of the kind shown in Fig. 11 were examined by scanning electron microscopy. Figures 12 to 14 are appropriate micrographs. Figure 12 shows clear examples of the physical contact restraints that can persist at an otherwise widely opened crack interface. Figure 13 presents a slightly more complex picture. Here the grains in the centers of the fields of view have developed secondary microfractures in the base region of attachment to one of the crack walls. There is a strong element of transgranular failure associated with this microfracture process, particularly evident in Fig. 13(*A*). Lastly, Fig. 14 illustrates a case in which a bridging grain has broken away from both walls and is presumably on the verge of detachment from the interface. Indeed, some minor fragments of material have already been thrown off as fracture debris, notably at lower left of the micrograph.

As with the cantilever beam specimens, evidence was sought that might reveal the presence of an extended frontal microcracking zone about the tips of arrested primary cracks in the strength specimens. Again, no such evidence was found in the SEM observations.

IV. Discussion

We have looked closely, at the microstructural level, into the processes of crack restraint in a coarse-grained alumina. This material, although ostensibly a simple, nontransforming ceramic, shows strong *R*-curve characteristics. Our observations provide clear evidence for grain-localized bridges at the newly formed crack interface behind the tip. These observations tie in with the sawcutting experiments of Knehans and Steinbrech[11] (Section I),

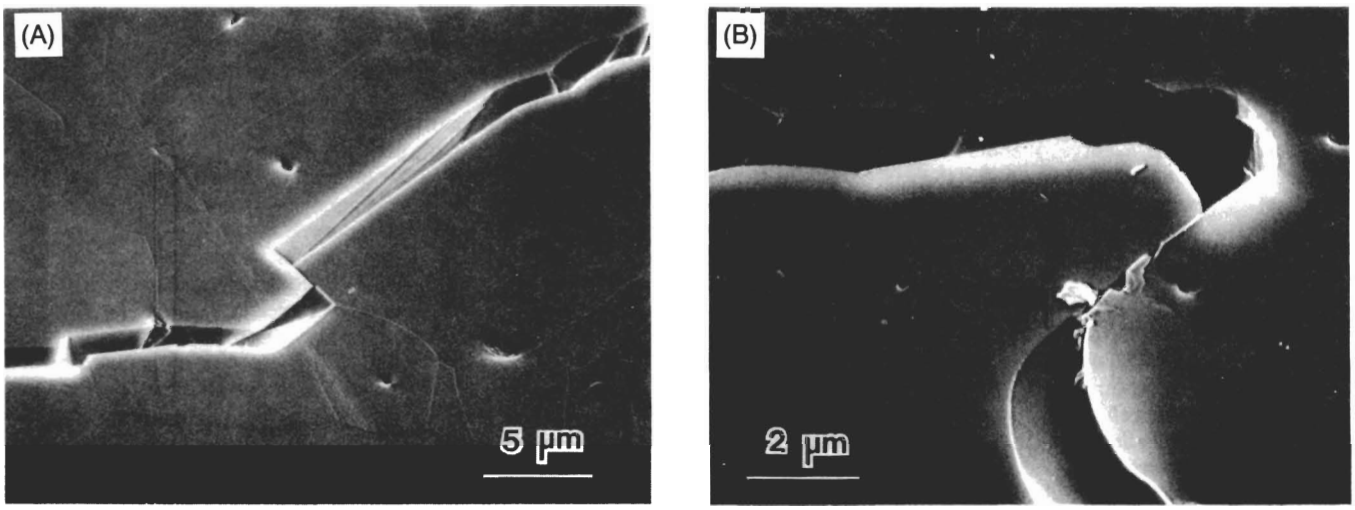

Fig. 12. Scanning electron micrographs of fractured-but-intact alumina disk, showing examples of apparent frictional interlocking at grain bridging sites.

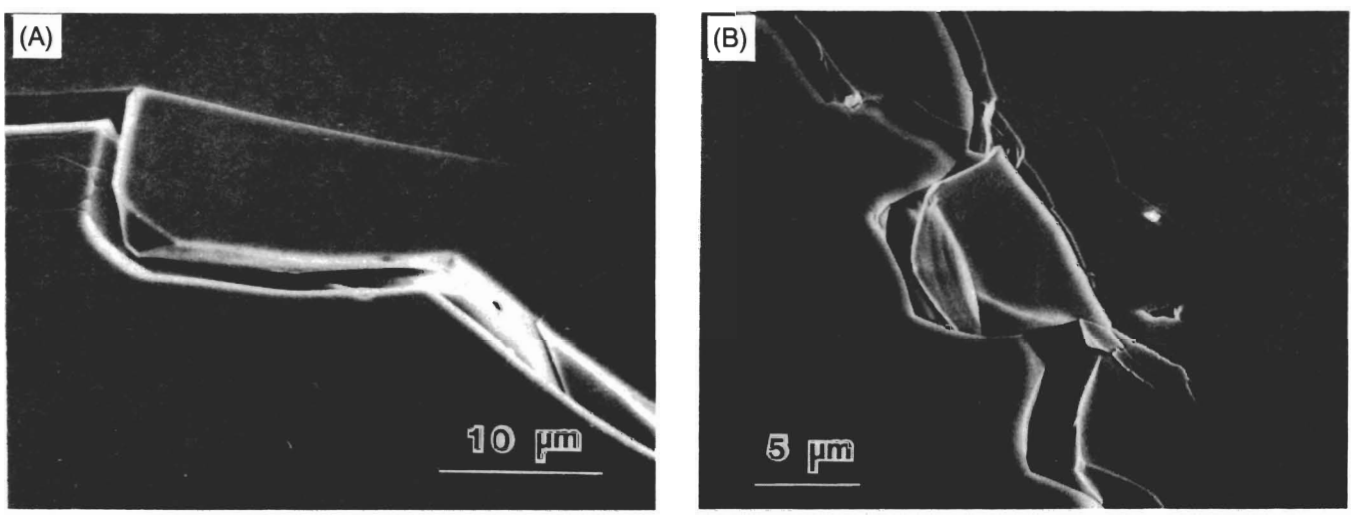

Fig. 13. Scanning electron micrographs, showing secondary microfracture about bridging grains, indicating the intensity of interface traction forces.

in which the crack wake was identified as the crucial source region for the *R*-curve behavior. Here, in situ experiments have proved most informative, revealing features in the crack response that are not at all apparent from the usual post-mortem (or even interrupted) tests. Not only is the growth highly stable, typical of a rapidly rising toughness characteristic, but it is discontinuous on the microscale. Associated with this discontinuity is the appearance of segmented fracture traces at the specimen surfaces. However, these segments connect beneath the surface into a common, primary crack interface. We picture these discrete, incipient grain bridging sites as uniformly distributed in the projected fracture plane. As the fracture front advances, the grain bridging sites are left behind and provide a restraining force which must ultimately be overcome for failure to occur.

It is well to reemphasize at this point that the notion of a physically restrained crack interface is not exactly revolutionary. Many years ago Hoagland *et al.*,[27] in a metallographic sectioning study, presented much the same picture for the brittle fracture of *steels*. Again, Hillerborg *et al.*[36] and others in the *concrete* literature have been considering the prospect of bridging mechanisms for a decade or so. More recently, one of us[18,19] has identified analogous mechanisms (using in situ video recording units, acoustic emission location techniques, etc.) in geological *rock* specimens. There is

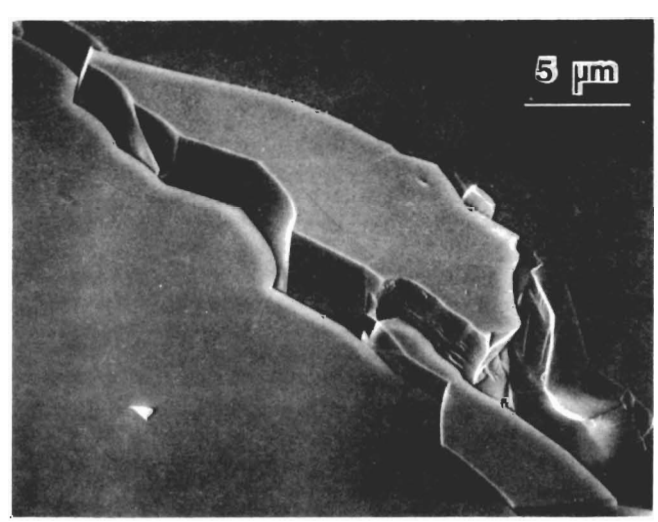

Fig. 14. Scanning electron micrograph, showing detachment of bridging grain from fracture interface.

therefore plenty of evidence to suggest that this is a general phenomenon. As far as the present study goes, our focus on alumina does not allow us to extend this generalization to other ceramics. However, some preliminary observations on other ceramic systems in these laboratories, e.g., glass-ceramics, along with the implied universality in the *R*-curve phenomenology from the earlier, broader-based indentation-strength study[20,21] (see Section I), indicate that the interface-bridging mode may be far more widespread than hitherto suspected.

Although there appears to be little doubt about the *location* of the toughening agents in our material, the *nature* of the actual separation process remains somewhat obscure. We have presented compelling evidence for the continual development of secondary fractures, accompanied by frictional tractions, around bridging grains, confirming in large part a mechanism foreshadowed by Knehans and Steinbrech and co-workers.[14,15] However, what we have *not* been able to determine is the specific form of the discrete force-separation function that defines the micromechanics of the bridge rupture event. About all that we might say about this function is that it probably has a pronounced tail, bearing in mind the persistent activity at the bridging sites in Figs. 4 to 6 (in some cases long after one or the other of the overlapping crack segments appears to have linked up with the primary fracture surface).

The present study, in addition to identifying a most likely source of toughening in nontransforming ceramics, calls into question the validity of practically all alternative models. Recall our earlier assertion (Section I) that the evidence cited in favor of these alternative models in the literature is almost invariably circumstantial, based at best on post-mortem fractography. The popular notion of a profuse frontal microcracking zone is a prime case in point. We are unaware of any direct observation of such a zone about a growing crack in any nontransforming ceramic material (although there are some recent indications that microcracking may have a role to play in *transforming, multiphase* ceramics[28]). Our own observations gave no indication of dispersed microcracking (other than the bridging grain secondary fractures immediately adjacent to the crack walls). Yet according to the frontal-zone models[7] we would expect events in the alumina to be observable as far distant as several millimeters from the crack interface (Appendix). Moreover, one would expect to find these events manifested cumulatively as a general uprising of material adjacent to the crack trace on the free surface of the fracture specimens, since it is via a predicted dilatancy that the microcracking makes its predominant contribution to the toughening.[7] Striking examples of this kind of uprising have in fact been reported in studies on zirconia,[29,30] where the dissipation-zone description is beyond dispute. Again, the ceramics profilometry examinations revealed nothing (at least within the resolution limit of the profilometer) to support the dilatancy argument in the alumina studied here.

Reference was made in Section I to another possible model, based on crack-tip/internal-stress interactions, for explaining the *R*-curve behavior. At first sight this model does appear to be able to account for most important features of the *R* curve, especially the long range in crack sizes (relative to the grain structure) over which the toughness rises; it is argued that the microscale cracks are most likely to experience the full effect of local tensile forces but that, as extension proceeds, the cracks should gradually average out over alternative tensile and compressive grain elements.[8] However, if this were to be the whole story, the toughness of our polycrystalline alumina should saturate out at the grain boundary energy, so that, since the grain boundary is weaker than the matrix single crystal (for otherwise the fracture would be transgranular), the saturated toughness could never exceed that of sapphire. This is inconsistent with the previous indentation-strength study, where the strength-load[20] (or equivalently, toughness-load[22]) curves for polycrystalline alumina and single-crystal sapphire cross each other. Moreover, the internal stress model cannot explain the observation of *R*-curve behavior in specimens with large starter notches; the stress-averaging effect is necessarily already complete in such large crack configurations. Of course, the possibility remains that these same internal stresses could play a secondary role, by acting in concert with some other toughening mechanism; again, the absence of any abrupt increases in the crack resistance curve (i.e., on the scale of the microstructure itself) excludes certain mechanisms, e.g., deflection, pinning and bowing, as potential partners. Whether internal stresses have anything to do with the bridging mechanism advocated here, e.g., by establishing suitable conditions for creating the ligamentary elements in the first place, is a possibility that might well be explored.

In summary, our observations provide strong, direct evidence for grain-localized bridging elements as a principal source of *R*-curve behavior in nontransforming ceramics. The actual physical separation process involves secondary cracking and frictional interlocking, but the detailed micromechanics remain obscure. We have nevertheless managed to obtain some feeling for the critical dimensions involved in this process for the alumina used here. In particular, we gauge the mean bridge spacing, as reflected by the scale of discontinuous crack growth, to be $\approx$2 to 3 grain diameters, and the interfacial traction-zone length behind the crack tip to be $\gtrsim$100 grain diameters. These dimensions will serve as a basis for our fracture mechanics modeling in Part II.

APPENDIX

Evans and Faber[7] provide a formulation of the frontal microcrack zone model from which we can estimate the spatial extent of any microcracking. Assuming that the primary-crack/microcrack interaction arises principally from an averaged dilatancy within the frontal zone, yet (to a first approximation) without perturbing the stress field outside the zone, these authors take the zone width (measured perpendicular to the crack plane) as

$$h = [3^{1/2}(1 + \nu^2)^2/12\pi](K^\infty/\sigma_c)^2$$

where ν is Poisson's ratio, K^∞ is the stress intensity factor associated with the applied field, and σ_c is the critical local stress for microcrack initiation. Inserting $\nu = 0.22$, $K^\infty = 6.5$ MPa·m$^{1/2}$ (saturation toughness, see Part II), and $\sigma_c = 20$ MPa (estimate from Evans and Faber), we obtain $h \approx 5$ mm for our alumina.

Acknowledgments: The authors gratefully acknowledge stimulating discussions with R. F. Cook, E. R. Fuller, F. F. Lange, D. B. Marshall, R. Steinbrech, and M. V. Swain during the course of this work. T. Vorburger performed the profilometer traces.

References

[1]Y.-W. Mai and B. R. Lawn, "Crack Stability and Toughness Characteristics in Brittle Materials," *Ann. Rev. Mater. Sci.*, **16**, 415–39 (1986).
[2]D. Broek; Chs. 5 and 8 in Elementary Fracture Mechanics. Martinus-Nijhoff, Boston, 1982.
[3]R. C. Garvie, R. H. Hannink, and R. T. Pascoe, "Ceramic Steel," *Nature (London)*, **258** [5537] 703–704 (1975).
[4]Advances in Ceramics, Vol. 3, Science and Technology of Zirconia. Edited by A. H. Heuer and L. W. Hobbs. American Ceramic Society, Columbus, OH, 1981.
[5]R. A. McMeeking and A. G. Evans, "Mechanics of Transformation Toughening in Brittle Materials," *J. Am. Ceram. Soc.*, **65** [2] 242–46 (1982).
[6]R. G. Hoagland and J. D. Embury, "A Treatment of Inelastic Deformation Around a Crack Tip Due to Microcracking," *J. Am. Ceram. Soc.*, **63** [7–8] 404–10 (1980).
[7]A. G. Evans and K. T. Faber, "Crack Growth Resistance of Microcracking Brittle Materials," *J. Am. Ceram. Soc.*, **67** [4] 255–60 (1984).
[8]R. W. Rice, R. C. Pohanka, and W. J. McDonough, "Effect of Stresses from Thermal Expansion Anisotropy, Phase Transformations, and Second Phases on the Strength of Ceramics," *J. Am. Ceram. Soc.*, **63** [11–12] 703–10 (1980).
[9]F. F. Lange, "The Interaction of a Crack Front with a Second-Phase Dispersion," *Philos. Mag.*, **22**, 983–92 (1970).
[10]K. T. Faber and A. G. Evans, "Crack Deflection Processes: I. Theory; II. Experiment," *Acta Metall.*, **31** [4] 565–76, 577–84 (1983).
[11]R. Knehans and R. Steinbrech, "Memory Effect of Crack Resistance During Slow Crack Growth in Notched Al_2O_3 Specimens," *J. Mater. Sci. Lett.*, **1** [8] 327–29 (1982).
[12]A. G. Evans, A. H. Heuer, and D. L. Porter; pp. 529–56 in Fracture 1977, Vol. 1. Edited by D. M. R. Taplin. University of Waterloo Press, Ontario, Canada, 1977.
[13]H. Hubner and W. Jillek, "Subcritical Crack Extension and Crack Resistance in Polycrystalline Alumina," *J. Mater. Sci.*, **12** [1] 117–25 (1977).
[14]R. Knehans and R. Steinbrech, "Effect of Grain Size on the Crack Resistance Curves of Al_2O_3 Bend Specimens," *Sci. Ceram.*, **12**, 613–19 (1983).
[15]F. Deuerler, R. Knehans, and R. Steinbrech, "Testing Methods and Crack Resistance Behavior of Al_2O_3"; to be published in *Sci. Ceram.*, Vol. 13.
[16]A. Hillerborg, M. Madeer, and P. E. Peterson, "Analysis of Crack Formation and Crack Growth in Concrete by Means of Fracture Mechanics and Finite Elements." *Cem. Concr. Res.*, **6** [6] 773–82 (1976).
[17]M. Wercharatana and S. P. Shah, "Prediction of Nonlinear Fracture Process Zone in Concrete," *J. Eng. Fract. Mech.*, **109** [5] 1231–46 (1983).
[18]P. L. Swanson, "Subcritical Fracture Propagation in Rocks: An Examination Using the Methods of Fracture Mechanics and Non-Destructive Testing"; Ph.D.

Thesis. University of Colorado, Boulder, CO, 1984.
[19]P. L. Swanson; pp. 299–317 in Fracture Mechanics of Ceramics, Vol. 8. Edited by R. C. Bradt, A. G. Evans, D. P. H. Hasselman, and F. F. Lange. Plenum, New York, 1986.
[20]R. F. Cook, B. R. Lawn, and C. J. Fairbanks, "Microstructure-Strength Properties in Ceramics: I. Effect of Crack Size on Toughness," *J. Am. Ceram. Soc.*, **68** [11] 604–15 (1985).
[21]R. F. Cook, B. R. Lawn, and C. J. Fairbanks, "Microstructure-Strength Properties in Ceramics: II. Fatigue Relations," *J. Am. Ceram. Soc.*, **68** [11] 616–23 (1985).
[22]C. J. Fairbanks, B. R. Lawn, R. F. Cook, and Y.-W. Mai; pp. 23–37 in Fracture Mechanics of Ceramics, Vol. 8. Edited by R. C. Bradt, A. G. Evans, D. P. H. Hasselman, and F. F. Lange. Plenum, New York, 1986.
[23]R. F. Cook, C. J. Fairbanks, B. R. Lawn, and Y.-W. Mai; to be published in *J. Mater. Res.*
[24]D. B. Marshall, "An Improved Biaxial Flexure Test for Ceramics," *Am. Ceram. Soc. Bull.*, **59** [5] 551–53 (1980).
[25]P. L. Swanson, "Tensile-Fracture Resistance Mechanisms in Brittle Polycrystals: An Ultrasonics and In-Situ Microscopy Investigation"; unpublished work.
[26]D. B. Marshall, B. R. Lawn, and P. Chantikul, "Residual Stress Effects in Sharp-Contact Cracking: II. Strength Degradation," *J. Mater. Sci.*, **14** [9] 2225–35 (1979).
[27]R. G. Hoagland, A. R. Rosenfeld, and G. T. Hahn, "Mechanisms of Fast Fracture and Arrest in Steels," *Metall. Trans.*, **3** [1] 123–35 (1972).
[28]M. Rühle, N. Claussen, and A. H. Heuer, "Transformation and Microcrack Toughening as Complementary Processes in ZrO_2-Toughened Al_2O_3," *J. Am. Ceram. Soc.*, **69** [3] 195–97 (1986).
[29]M. V. Swain and R. H. J. Hannink; pp. 225–39 in Advances in Ceramics, Vol. 12, Science and Technology of Zirconia II. Edited by N. Claussen, M. Rühle, and A. H. Heuer. American Ceramic Society, Columbus, OH, 1985.
[30]D. B. Marshall, "Strength Characteristics of Transformation-Toughened Zirconia," *J. Am. Ceram. Soc.*, **69** [3] 173–80 (1986). □